Journal of Pharmaceutical and Biomedical Analysis 219 (2022) 114912

Contents lists available at ScienceDirect

Journal of Pharmaceutical and Biomedical Analysis

journal homepage: www.journals.elsevier.com/journal-of-pharmaceutical-and-biomedical-analysis

Macrocyclic glycopeptides- and derivatized cyclofructan-based chiral stationary phases for the enantioseparation of fluorinated β-phenylalanine analogs

Dániel Tanács [a], Róbert Berkecz [a], Sayeh Shahmohammadi [b], Enikő Forró [b], Daniel W. Armstrong [c], Antal Péter [a], István Ilisz [a,*]

[a] Institute of Pharmaceutical Analysis, Interdisciplinary Excellence Centre, University of Szeged, Somogyi u. 4, H-6720 Szeged, Hungary
[b] Institute of Pharmaceutical Chemistry, University of Szeged, Eötvös u. 6, H-6720 Szeged, Hungary
[c] Department of Chemistry and Biochemistry, University of Texas at Arlington, Arlington, TX 76019-0065, USA

ARTICLE INFO

Keywords:
Superficially porous particles
Enantioselective separation
Macrocyclic glycopeptide-based chiral stationary phases
Cyclofructan-6-based chiral stationary phases
Fluorinated β-phenylalanines

ABSTRACT

The enantioseparation of five fluorinated β-phenylalanine analogs together with the nonfluorinated α- and β-phenylalanines has been investigated utilizing chiral stationary phases. The employed chiral selectors include macrocyclic antibiotics, such as vancomycin, teicoplanin, and teicoplanin aglycone, isopropyl carbamate functionalized cyclofructan-6, and *Cinchona* alkaloid-based *tert.*-butyl carbamate quinine, all covalently bonded to 2.7 μm superficially porous silica particles. The applied conditions included reversed-phase and polar-ionic modes where the vancomycin-, and the cyclofructan-6-based core-shell particles proved to offer suitable efficiency. Under reversed-phase conditions typical hydrophobic chromatographic behavior was observed, especially in the H_2O/MeOH system. The improved selectivity with increasing MeOH content observed in polar ionic mode suggests that H-bonding may not play a major role in the chiral recognition. The stoichiometric displacement model was probed to gather information on the ionic interactions. The ion-exchange process was found to affect retention, but it has no essential contribution to chiral recognition. Without paying special attention to the optimization of the system volume of the UHPLC instrument plate heights varying in the range of 10–50 μm were obtained. In all cases, retention and selectivity decreased with increasing temperature, and enthalpy-driven enantiorecognition was observed. Elution sequences were determined in all cases.

1. Introduction

Enantiomerically pure β-aryl-substituted β-amino acids are important compounds from both biological and chemical aspects and are widely investigated in drug research [1]. Some are used in the synthesis of novel antibiotics [2] and analgesic endomorphin-1 analog tetrapeptides [3]. Owing to the significantly different characteristics of the C–F bond, replacing one or more hydrogen atoms in a compound by fluorine, a considerable difference in biological activity can be expected. Due to their importance in the design and synthesis of potential pharmaceutical drugs fluorinated amino acids have gained increasing attention [4]. For example (±)-eflornithine is used for the treatment of trypanosomiasis [5] and facial hirsutism in women [6]. To be able to determine enantiomeric purities and to optimize the synthetic routes using fluorinated precursor molecules, *i.e.* chiral synthons, enantioselective separation assays must be developed.

The various possibilities for direct stereoselective analyses of chiral molecules, including amino acids, have been reviewed in many papers and book chapters [7,8]. Despite the vast literature chiral analysis, examples of liquid chromatography-based enantioselective separations of fluorinated amino acids are limited. In the early 2000s, ligand-exchange micellar capillary chromatography was applied for the enantioseparation of fluorine-substituted phenylalanine analogs [9], while stereoisomers of nonproteogenic polyfluoroamino acids and peptides were resolved on Chiralcel OD-H [10]. For the enantioseparation of five -NHBoc and -CO_2Et protected fluorinated cyclic β^3-amino acid analogs and their nonfluorinated counterparts polysaccharide-based chiral stationary phases (CSPs) were applied [11]. Very recently *Cinchona* alkaloid-based zwitterionic CSPs have been successfully utilized for the enantioseparation of fluorinated β-phenylalanine derivatives [12].

* Correspondence to: Institute of Pharmaceutical Analysis, University of Szeged, Somogyi B. u. 4, H-6720 Szeged, Hungary.
E-mail address: ilisz.istvan@szte.hu (I. Ilisz).

https://doi.org/10.1016/j.jpba.2022.114912
Received 5 April 2022; Received in revised form 20 June 2022; Accepted 23 June 2022
Available online 26 June 2022

In SFC due to the lower eluent viscosity columns with smaller particle sizes have become more widespread [13–15]. However, today numerous liquid phase enantioselective separations are being carried out on traditional HPLC systems, utilizing typically chiral columns of fully porous particles (FPPs) of 5 μm. Thanks to the efficient functionalization of the selector molecules and the development of silica technology, a new generation of chiral columns based on core-shell particles (superficially porous particles, SPPs) and sub-2 μm FPPs opened a promising perspective in "chiral" liquid chromatography. Due to the intensive work of different research groups the most frequently applied chiral selectors were bonded to SPPs or FPPs resulting in very effective CSPs. Armstrong et al. [16] and Gasparrini et al. [17] used macrocyclic glycopeptides (teicoplanin, teicoplanin aglycone, vancomycin) for immobilization, while functionalized cyclofructans were linked to SPP and FPP support by Armstrong et al. [16,18]. Functionalized polysaccharides on SPP and FPP support were first applied by Chankvetadze et al. [19], while *Cinchona* alkaloid-based mono- and zwitterionic CSPs applying SPPs and FPPs was developed by Armstrong et al. [20] and Lämmerhofer et al. [21], respectively. It is worth noting that in addition to the above citations, some very recent review papers have summarized these new results [22–24].

The aims of this work are to explore the chromatographic behavior of fluorine-containing compounds of pharmaceutical relevance and to characterize the CSPs from both a kinetic and thermodynamic point of view. Another goal of this study was to develop methods using high-efficiency core-shell particles for liquid chromatography-based enantioselective separation of five fluorinated β-phenylalanine analogs and the nonfluorinated α- and β-phenylalanines. Applying both reversed-phase (RP) and polar-ionic (PI) mobile phase systems permitted evaluation of the effects of bulk solvent composition, the nature, and concentration of various mobile phase components in the reversed-phase mode (RPM). This study focuses on general tendencies resulting from the structural peculiarities of the pharmacologically interesting fluorinated analytes, in the context of their enantioseparation on different core-shell particle-based CSPs. Evaluation of van Deemter plots provided a basis for the kinetic behavior while a separate thermodynamic characterization is also an integral part of this study. Knowing the absolute configuration of all the studied enantiomers their elution sequences also were determined.

2. Materials and methods

2.1. Chemicals and materials

Structures of the studied analytes are shown in Fig. 1. (*S*)- and (*R*)-phenylalanine (**1**) was purchased from Sigma–Aldrich (St Louis, MO, USA). Racemic amino acid **2** was prepared through ring cleavage of racemic 4-phenylazetidin-2-one with 18% HCl [25], while **3–7** were synthesized through condensation of the corresponding aldehydes with malonic acid in the presence of NH_4OAc in EtOH [26]. CAL-B (*Candida antarctica* lipase B)-catalyzed ring cleavage of 4-phenylazetidin-2-one resulted in phenyl-substituted β-amino acid (*S*)-**2** with excellent *ee* ($\geq$ 99%) [25]. Enantiomeric fluorophenyl-substituted β-amino acids (*S*)-**3–7** (*ee* $\geq$ 99%) were prepared through lipase PSIM (*Burkholderia cepacia*)-catalyzed hydrolysis of the corresponding racemic β-amino carboxylic ester hydrochlorides [26].

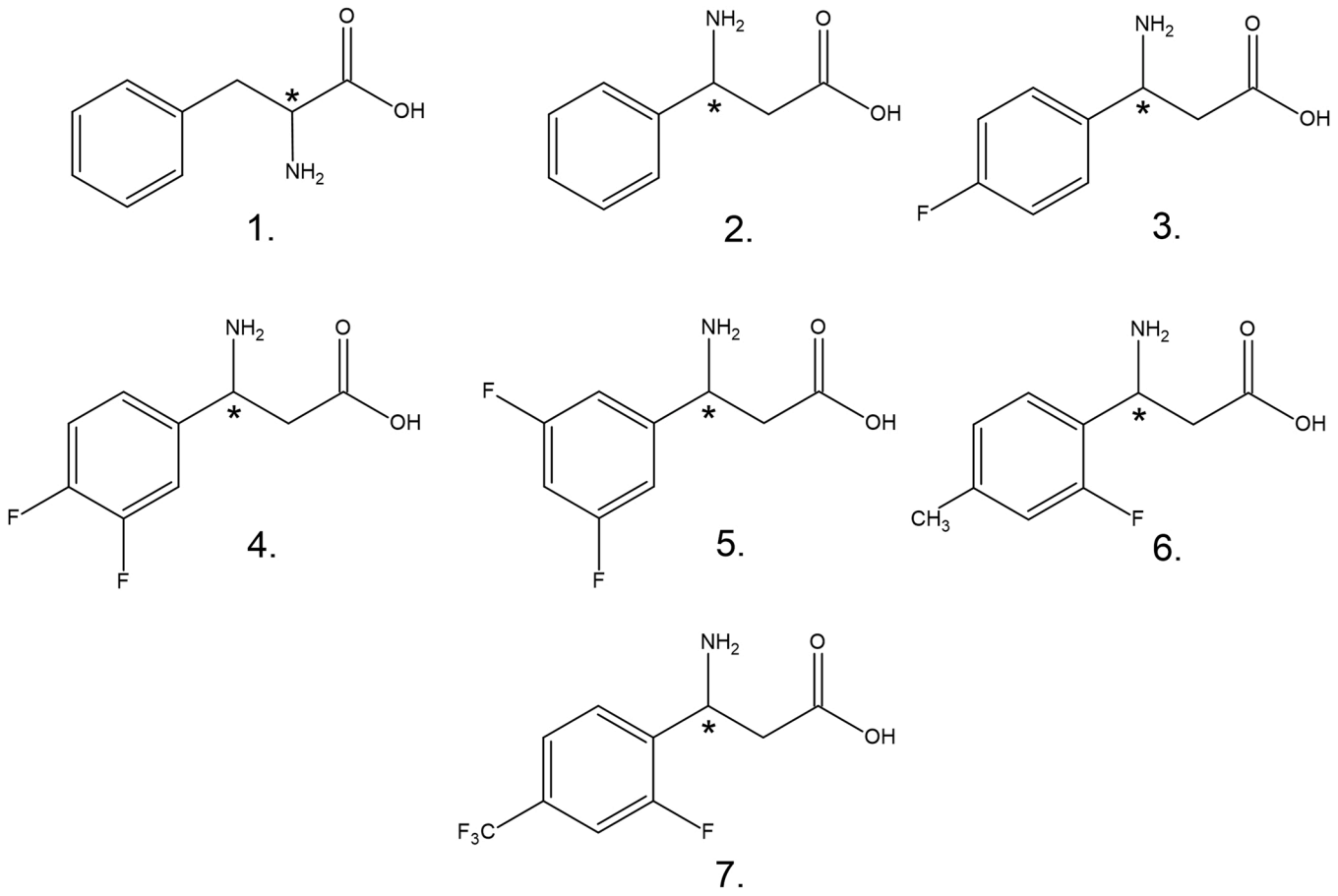

Fig. 1. Structure of analytes**, 1,** phenylalanine; **2,** 3-amino-3-phenylpropanoic acid; **3,** 3-amino-3-(4-fluorophenyl)propanoic acid; **4,** 3-amino-3-(3,4-difluorophenyl) propanoic acid; **5,** 3-amino-3-(3,5-difluorophenyl)propanoic acid; **6,** 3-amino-3-(2-fluoro-4-methylphenyl)propanoic acid; **7,** 3-amino-3-[2-fluoro-4-(trifluoromethyl) phenyl]propanoic acid.

Methanol (MeOH), acetonitrile (MeCN), and water of LC-MS grade, NH_3 dissolved in MeOH, triethylamine (TEA), formic acid (FA), glacial acetic acid (AcOH), and ammonium acetate (NH_4OAc) of analytical reagent grade were from VWR International (Radnor, PA, USA).

2.2. Apparatus and chromatography

The applied Waters® ACQUITY UPLC® H-Class PLUS UHPLC System with Empower 3 software (Waters Incorporation, Milford, MA, USA) consisted of a quaternary solvent manager, sample manager FTN-H, column manager, PDA detector, and QDa mass spectrometer detector.

Chiral selectors, used in this study are attached covalently to 2.7 μm silica-based SPPs. The core diameter and shell thickness of the SPPs were 1.7 μm and 0.5 μm, respectively. All columns have 100 × 3.0 mm i.d. or 100 × 2.1 mm i.d. dimensions (abbreviations for i.d. dimensions are: **3.0** and **2.1**, respectively). Selectors of macrocyclic glycopeptide-based columns are vancomycin (VancoShell, **V-3.0**, and **V-2.1**), teicoplanin (TeicoShell, **T-3.0** and **T-2.1**), teicoplanin aglycone (TagShell, **Tag-3.0**, and **Tag-2.1**). Isopropyl carbamate functionalized cyclofructan-6 (**CF6-P-3.0** and **CF6-P-2.1**) and *Cinchona* alkaloid-based *tert.*-butyl carbamate quinine (**Q-Shell, Q-3.0**) were also employed. All columns were obtained from AZYP (LLC, Arlington, TX, USA).

Stock solutions of analytes (1.0 mg ml^{-1}) were prepared in MeOH and diluted with the mobile phase. The hold-up time (t_0) of the columns was determined by 0.1% AcOH dissolved in MeOH and detected at 210 or 256 nm. The flow rate was set at 0.3 ml min^{-1}, which provided suitable efficiency for both column dimensions, and the column temperature at 20 °C (if not otherwise stated).

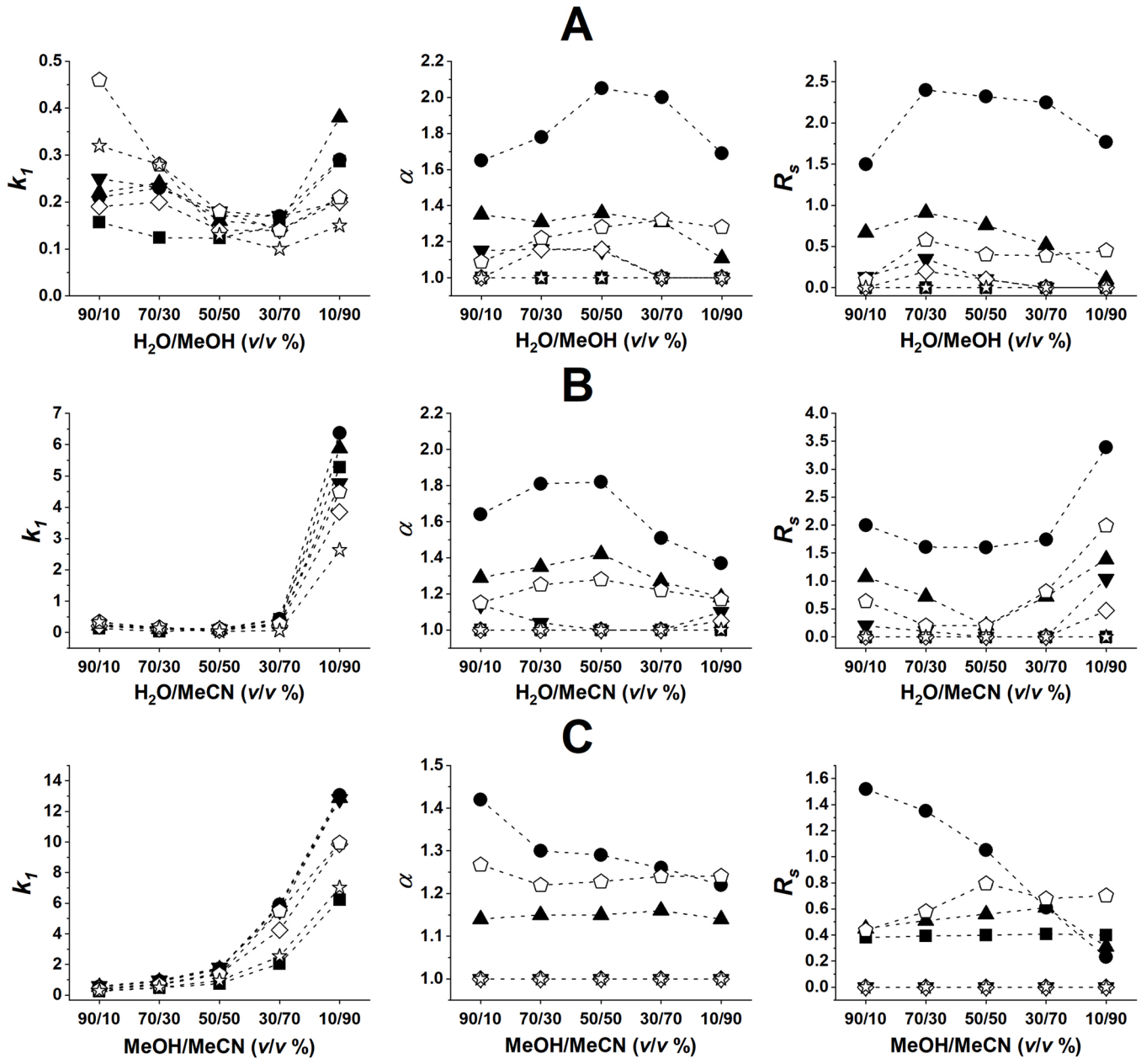

Fig. 2. Effect of bulk solvent composition on retention factor of first eluting enantiomer (k_1), separation factor (α), and resolution (R_S) on VancoShell CSP**,** Chromatographic conditions: column, VancoShell (**V-3.0**); mobile phase, **A**, H_2O/MeOH, 90/10–10/90 (*v/v*) containing 0.1% TEAA, **B**, H_2O/MeCN, 90/10–10/90 (*v/v*) containing 0.1% TEAA, **C**, MeOH/MeCN, 90/10–10/90 (*v/v*) containing 0.1% TEAA; detection, 215 nm; flow rate, 0.3 ml min^{-1}; temperature, 20 °C; symbols, analyte **1,** ■; **2,** ● **3,** ▲; **4,** ▼; **5,** ⋄; **6,** ⬠; and **7,** ☆.

3. Results and discussion

3.1. Separation of phenylalanine analogs on macrocyclic glycopeptide-based CSPs

For the separation of amino acids, amines, and organic acids, macrocyclic glycopeptide-based CSPs can be applied in different chromatographic modes, however, the best performances are usually achieved in polar ionic mode (PIM) and RPM. Among macrocyclic antibiotics, teicoplanin and teicoplanin aglycone-based CSPs are most frequently used for the enantioseparation of α- and β-amino acids [23]. Preliminary experiments revealed unexpectedly that despite the variation of mobile phase composition the teicoplanin-based **T-3.0** CSP did not exhibit significant enantiorecognition ability either in RPM or PIM (data not shown). Under the same conditions, the teicoplanin aglycone-based **Tag-3.0** CSP exhibited some separation ability for a few fluorinated β-phenylalanines (*vide infra*), while the vancomycin-based **V-3.0** CSP provided the best results. Fig. 2 and Table S1 provide data for the separations achieved with **V-3.0** CSP using RP mobile phase systems of H_2O/MeOH (90/10–10/90 *v/v*) (Fig. 2 A) or H_2O/MeCN (90/10–10/90 *v/v*) (Fig. 2B), all containing 0.1%(*v/v*) TEAA. The retention factor of the first eluting enantiomer (k_1) exhibited curve minima with increasing MeOH or MeCN content in both eluent systems. With increasing water content, typical hydrophobic chromatographic behavior, especially in the H_2O/MeOH system was observed. The increased retentions observed at higher MeOH or MeCN content can be explained by the decreased solvation shell of the ionized analytes and selector as well as the decreased solubility of these analytes in organic solvents. Interestingly, at high MeCN content, an order of magnitude higher k_1 values were observed compared to MeOH. The solvation (solubility) of ionized analytes in polar but aprotic MeCN is less favored, resulting in increased retention. The lowest k_1 values were obtained between 50% and 70%(*v/v*) MeOH or MeCN content of the RP mobile phase. Typically, selectivity peaked at 30–50%(*v/v*) organic content in the mobile phase, then decreased. Resolution values in the H_2O/MeOH system displayed similar α value trends in that they displayed maxima. In the H_2O/MeCN system, R_S values exhibited minimum curves with the highest R_S values registered at the highest MeCN content.

In PIM a mixture of MeOH (possessing polar and protic properties) and MeCN (as polar but aprotic solvent) together with acid and base additives are generally used. In PIM the MeOH/MeCN ratio was varied from 90/10–10/90 (*v/v*), and all mobile phases contained 0.1%(*v/v*) TEAA. As a result of the increase of MeCN content in the mobile phase, a significant increase in retention factors was obtained for all analytes (Fig. 2 C). At high MeCN content, the solvation of polar amino acids in the aprotic solvent decreases markedly resulting in high retentions, while the increasing ratio of protic MeOH favors the solvation of polar amino acids, *i.e.*, retention decreases. The stronger interaction with the CSP was not associated with enhanced enantiorecognition; α and R_S generally were greater at higher MeOH contents, especially for analyte **2**. The improved selectivity with increasing MeOH content suggests that H-bonding may not play a major role in these enantioseparations.

As mentioned earlier, in the case of the teicoplanin aglycone-based CSP (**Tag-3.0**) moderate enantiorecognition could be achieved for some analytes. Applying the same eluent systems as for **V-3.0**, analytes **1**, **6**, and **7** could at least partially be enantioseparated (Fig. S1). The trends in the change of k_1, α, and R_S values are similar to those observed on the **V-3.0** column. Interestingly, the two CSPs with different structures exhibited complementary properties to the enantioselective recognition of α- and β-phenylalanine. Namely, α-phenylalanine could be effectively enantioseparated with **Tag-3.0**, but not with **V-3.0**, while β-phenylalanine with **V-3.0**, but not with **Tag-3.0**. Based on this observation the importance of steric contributions in the chiral recognition process is probable.

3.2. Evaluation of the stoichiometric displacement model

Both vancomycin- and teicoplanin aglycone-based selectors contain carboxyl and primary amino groups available for the ionic interactions with the amino or carboxyl group of the analyte. If ionic interactions have a determining role in the chiral recognition process it is supposed that the chromatographic ion-exchange mechanism can be described by the stoichiometric displacement model [27]. The model predicts a linear relationship between the logarithm of the retention factor and the logarithm of the counter-ion concentration for the retention behavior based on ion-pairing and ion-exchange mechanisms,

$$\log k = \log K_Z - Z \log c_{counter\text{-}ion}, \quad (1)$$

where Z is the effective charge (ratio of the charge number of the analytes and the counter-ions), while K_z describes the ion-exchange equilibrium. To check on the role of ionic interactions in the retention mechanism, the effects of counter-ion concentration on the chromatographic properties were examined on both **V-3.0** and **Tag-3.0** CSPs, applying optimized H_2O/MeOH, H_2O/MeCN, and MeOH/MeCN mobile phase conditions. In these experiments, the concentration of TEAA was varied in the range of 0.90–14.35 mM ensuring slightly acidic conditions, *i.e.,* the carboxyl group on both selector and select and could be present in deprotonated form, while the primary amino groups could be protonated. According to the data summarized in Fig. S2 with increased counter-ion concentration reduced retention is obtained. The linear fittings (plotting log k against log $c_{\text{counter-ion}}$) could be done with $R^2 > 0.98$ in all cases, where the slopes varied between –0.10 and –0.25 in the case of **V-3.0**, and between –0.01 and –0.11 in the case of **Tag-3.0** column. It is worth mentioning that on both CSPs, practically equal slopes were calculated for each enantiomer, *i.e.*, no significant difference could be observed in the enantioselectivities with varying counter-ion concentration (data not shown). Based on these findings it can be stated that in the studied chromatographic systems the ion-exchange process affects retention, but has no vital role in chiral recognition.

3.3. Separation of β-phenylalanine analogs on cyclofructane-6-based CSP

Cyclofructans (CFs) belong to the macrocyclic oligosaccharide family and are composed of 6 or more β-2,1 linked D-fructofuranose subunits [28]. It is important to note that the so-called CF6, containing six fructofuranose units does not have a central hydrophobic cavity, accordingly the formation of a hydrophobic inclusion complex (like in the case of cyclodextrins) is not possible. Their central core exhibits a similar structure as the 18-crown-6 crown ether, which is the reason why the chromatographic behavior resembles that of the crown ethers. Unlike the case of synthetic crown ethers, the amine group of the analyte does not have to be protonated and enantioselective interactions can occur in organic solvents and supercritical CO_2 rather than aqueous solvents [29].

Enantioseparations on cyclofructan-based CSPs generally are carried out in normal-phase mode and PIM [22]. Taking the solubility of amino acids into consideration, separations were carried out in the PIM using MeOH/MeCN as a bulk solvent in the presence of TFA and TEA as acid and base additives. Since the primary amino group and its interaction with core cyclofructan O-atoms play an important role in the enantiorecognition mechanism, first the effects of the concentration of acid, and the acid to base ratio were investigated. Fig. 3 A depicts the effects of the TFA/TEA ratio in the MeOH/MeCN 10/90 (*v/v*) mobile phase for the selected analytes **1**, **2**, **3**, and **7**. As can be seen in Fig. 3 A, k_1 slightly decreases with an increase in the TFA/TEA ratio, while α and R_S vary only slightly, but are usually somewhat better at *ca.* TFA:TEA 3:2 ratio. Keeping the TFA/TEA ratio at 3:2 their amount was varied between 0.15/0.10 (*v/v%*)–0.60/0.40 (*v/v%*) (Fig. 3B). With increasing TFA/TEA concentration k_1 slightly decreases, α does not change significantly, while R_S showed its maximum value at TFA:TEA 0.15:0.10 (*v/v%*) or

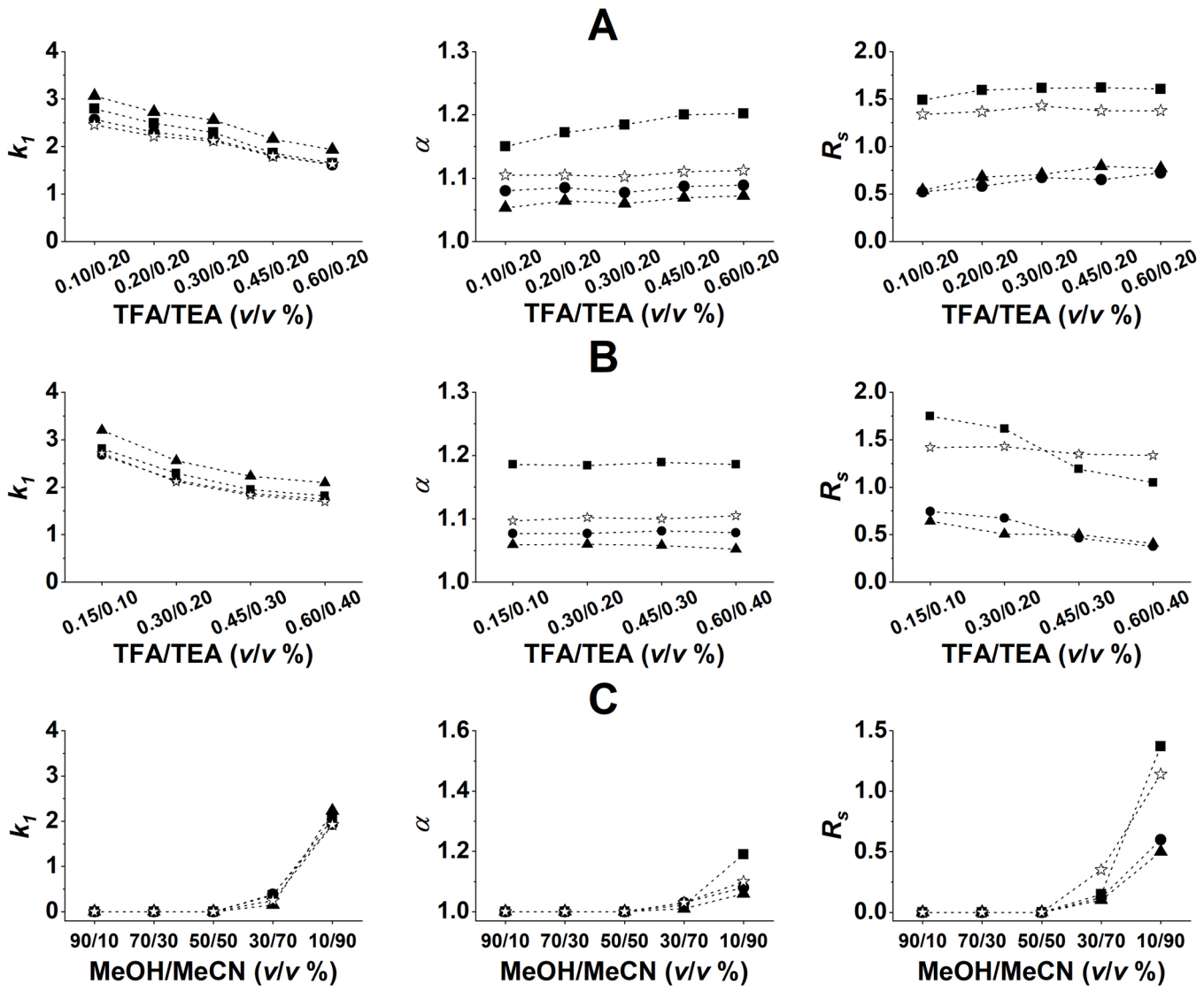

Fig. 3. Effect of **A,** TFA/TEA ratio, **B**, TFA/TEA concentration and **C**, MeOH/MeCN bulk solvent composition on retention factor of first eluting enantiomer (k_1), separation factor (α), and resolution (R_S) of analytes **1**, **2**, **3**, and **7** on LarihcShell-P CSP**,** Chromatographic conditions: column, LarihcShell-P (**CF6-P-3.0**); mobile phase, MeOH/MeCN, 10/90 (*v/v*) containing TFA/TEA in concentration of **A,** 0.10/0.20, 0.20/0.20, 0.30/0.20, 0.45/0.20 and 0.60/0.20 (*v/v%*), **B,** 0.15/0.10, 0.30/0.20, 0.45/0.30 and 0.60/0.40 (*v/v%*) and **C**, MeOH/MeCN, 90/10–10/90 (*v/v*) containing 0.3% TFA and 0.2% TEA; detection, 215 nm; flow rate, 0.3 ml min^{-1}; temperature, 20 °C; symbols, analyte **1**, ■; **2**, ● **3**, ▲; **4**, ▼; **5**, ◇; **6**, ⬡; and **7**, ☆.

0.30:0.20 (*v/v%*) concentration. TFA has a strong ion-pairing character and the trifluoroacetate-anion may interact with the protonated amino group of the amino acids. Therefore, less protonated amino groups are available for the interaction with O-atoms of the CF-6 ring, and retentions slightly decrease.

In the PIM the effect of bulk solvent composition was studied in a MeOH/MeCN 90/10–10/90 (*v/v*) mobile phase containing 0.3%(*v/v*) TFA and 0.2%(*v/v*) TEA. According to the data illustrated in Fig. 3 C, analytes were considerably retained only when the MeCN content exceeded 70%(*v/v*). The high concentration of aprotic MeCN hinders solvation of polar amino acids in the mobile phase leading to increased retention. As concerns α and R_S values, they behave differently than in the case of **V-3.0** CSP (Fig. 3 C *vs.* Fig. 2 C). The improved selectivity with increasing MeCN content suggests that stereoselective hydrogen bonding interactions between amino acids and isopropyl carbamate moiety of the selector take part in chiral recognition.

Functionalized *Cinchona* alkaloids (quinine and quinidine) are frequently applied for the chiral recognition of amino acid enantiomers [30–32]. For a set of experiments a CSP of *tert.*-butylcarbamate quinine immobilized on SPP support (Q-Shell, **Q-3.0**) was tested. A weak-anion exchange process between the protonated quinuclidine moiety of the chiral selector and the free carboxyl group of the analyte was assumed to take place. Contrary to our expectations, the **Q-3.0** CSP did not exhibit considerable enantiorecognition ability applying *aq.*NH_4OAc/MeOH mobile phase systems. Variation of H_2O/MeOH bulk solvent composition between 90/10–10/90 (*v/v*) containing 100 mM NH_4OAc revealed that k_1 increases significantly with increasing water content, but chiral recognition could not be achieved except for analytes **2** and **3** for which a partial separation was registered (data not shown).

As concerns elution sequences on macrocyclic glycopeptide phases $S < R$ was observed. However, on cyclofructan-6- and *Cinchona* alkaloid-based CSPs, the opposite, $R < S$ elution order was observed. Selected chromatograms for the chiral separation of enantiomers of the studied analytes are depicted in Fig. 4. Also, it should be noted that baseline enantiomeric separation of all these analytes can be achieved by lowering the temperature.

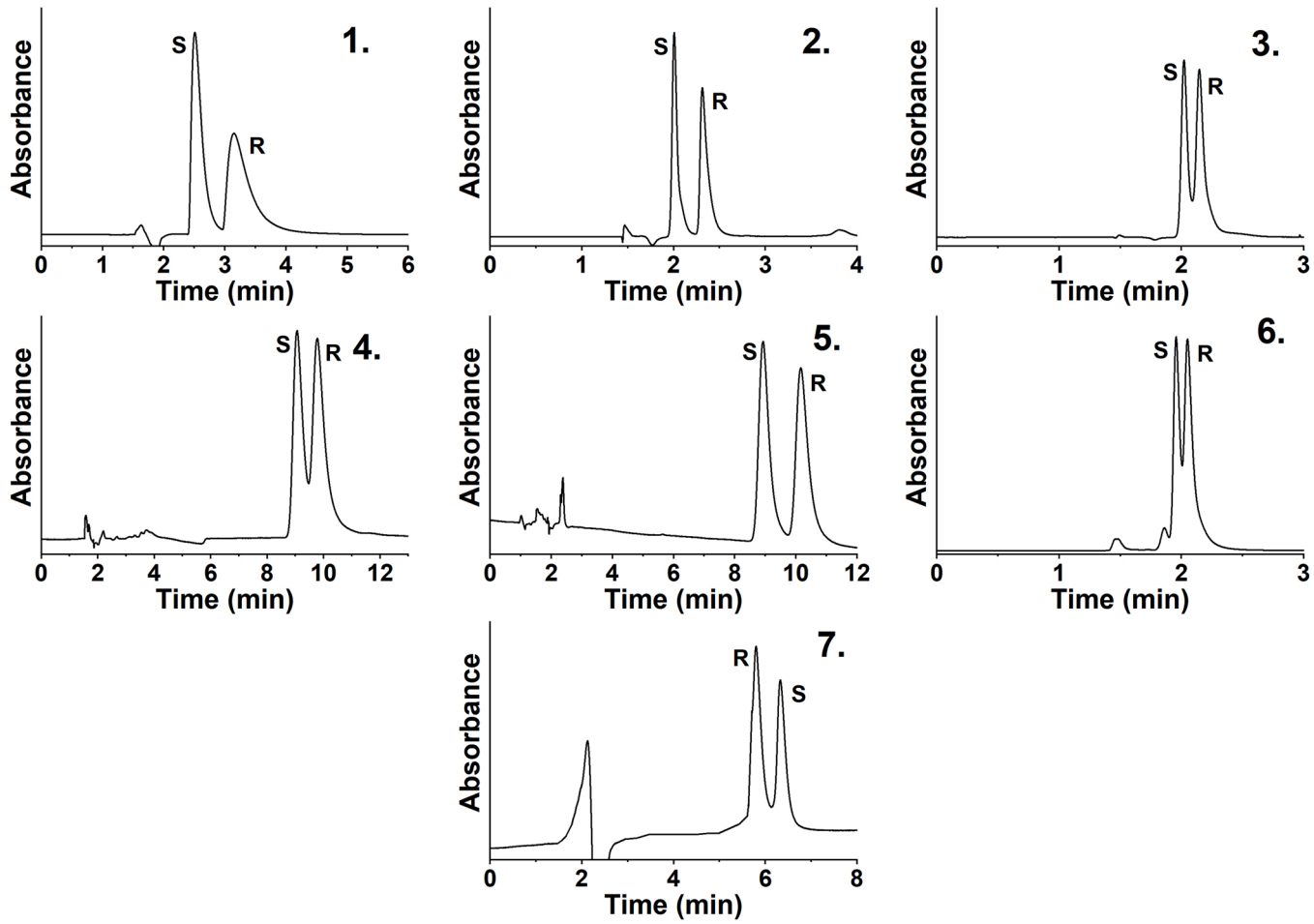

Fig. 4. Selected chromatograms Chromatographic conditions: column, for analyte 1,TagShell (Tag-3.0),for 2–6, VancoShell (V-3.0),and for 7,LarihcShell-P (CF6-P-3.0); mobile phase, for analyte 1 and 6, H2O/MeOH/TEAA, 10/90/0.1 (v/v/v), for 2 and 3, H2O/MeOH/TEAA 70/30/0.1 (v/v/v), for 4 and 5, H2O/MeCN/TEAA, 10/90/0.1 (v/v/v), and for 7, MeOH/MeCN 10/90 (v/v) containing 0.3 mM TFA and 0.2 mM TEA; detection, 215 nm; flow rate, 0.3 ml min-1; temperature, 20 °C.

3.4. van Deemter analysis

For the determination of van Deemter plots, mobile phases ensuring best separations and relatively low backpressures were selected. CSPs of both column dimensions (i.d. 3.0 and 2.1 mm) were studied to gain information about column kinetics.

In the case of VancoShell CSP a mobile phase of H_2O/MeCN 30/70 (*v/v*) containing 0.1%(*v/v*) TEAA (for analytes **2**, **3**, and **6)** was selected.

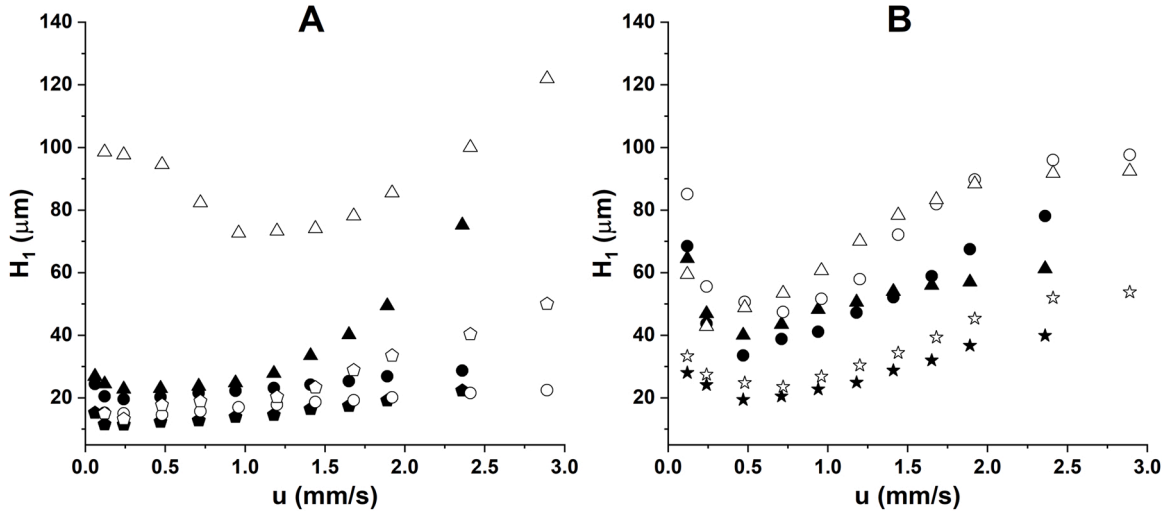

Fig. 5. van Deemter plots on VancoShell (**A**) and LarihcShell (**B**) CSPs**,** Chromatographic conditions: columns, **A,** VancoShell, **V-3.0** and **V-2.1**, and **B**, LarihcShell-P, **CF6-P-3.0** and **CF6-P-2.1**; mobile phase, **A,** H_2O/MeCN (30/70 *v/v*) containing 0.1% TEAA and **B**, MeOH/MeCN (10/90 *v/v*) containing 0.3 mM FA and 0.2 mM TEA; flow rate, 0.025 – 2.0 ml min^{-1}; detection, 256 nm; temperature, 20 °C; symbols, **A,** analyte **2, 3** and **6** on column V-3.0, ●, ▲, ⬟, respectively, and on column **V-2.1**, ○, △, □, respectively, and **B**, symbols, analyte **2**, **3**, and **7** on column **CF6-P-3.0**, ●, ▲, ★, respectively, and on column **CF6-P-2.1**, ○, △, ☆, respectively.

On **V-3.0** and **V-2.1** CSPs the curves for the first eluting enantiomer show a slight minimum for all studied analytes at ~0.2–0.3 mm sec^{-1} linear flow rate, however, this minimum for analyte **3** on **V-2.1** CSP was shifted to ~1.0–1.2 mm sec^{-1} (Fig. 5 A). Interestingly, for analyte **2** the H-u plot on the **V-2.1** column runs below the plot determined for **V-3.0**. It is worth noting that for analyte **3**, the H value for the first eluting enantiomer drastically increases with higher flow rates.

Van Deemter plots for analytes **2**, **3**, and **7** on LarihcShell-P CSPs were determined by using a mobile phase of MeOH/MeCN 10/90 (*v/v*) containing 0.3%(*v/v*) FA and 0.2%(*v/v*) TEA. On both **CF6-P-3.0** and **CF6-P-2.1** CSPs in the PIM, the curves for the first eluting enantiomer show characteristic minima at ~0.5 mm sec^{-1} linear flow rate (Fig. 5B). The H minima on **CF6-P-3.0** and **CF6-P-2.1** generally was higher than on **V-3.0** and **V-2.1** CSPs.

It should be mentioned that 2.1 mm i.d. columns were usually less efficient than the 3.0 mm ones for both types of selectors. This might be explained that column packing for the 2.1 mm is not ideal, compared to the 3.0 mm, however, wall effects may also contribute to worse efficiencies registered with the 2.1 mm columns. In this study we have not paid special attention to physically optimizing the UHPLC instrument for the measurements with the core-shell particle-based columns. The obtained plate heights (H_{min}) generally varied in the range of 10–50 μm. Comparing these results with the literature, it is clear that H_{min} very strongly depends on the nature of analytes, and similar examples can be found for other macrocyclic glycopeptide-based SPP CSPs [33,34]. The system volume of the UHPLC instrument was not optimized and lowering the extra-column effects may lead to a reduced H_{min} to some extent.

3.5. Thermodynamic characterization

In chiral separations, temperature effects on retention and selectivity can be evaluated using the van't Hoff equation in the form of

$$ln \quad \alpha = -\frac{\Delta(\Delta H^{\circ})}{RT} + \frac{\Delta(\Delta S^{\circ})}{R} \qquad (2)$$

here α is the selectivity factor, $\Delta(\Delta H^{\circ})$ and $\Delta(\Delta S^{\circ})$ are the differences in standard enthalpy and standard entropy, R is the universal gas constant, T is the temperature in degrees Kelvin. Utilizing Eq. 2, the problems related to the determination of the phase ratio can be excluded, however, the obtained thermodynamic parameters will still contain both enantioselective and nonselective contributions as discussed by Asnin and Stepanova [35].

The effects of temperature on chromatographic parameters were studied for analytes **2–6** on **V-3.0** (analytes **1** and **7** exhibited no separation on **V-3.0**) in the temperature range 5–50 °C. As discussed above, both in the RPM and PIM, retention and enantioselectivity depend on mobile phase composition. To explore how the changes in eluent composition affect the thermodynamic temperature dependence, studies were carried out with different mobile phase compositions. In RPM H_2O/MeOH 70/30 and 10/90 (*v/v*), and H_2O/MeCN 70/30 and 10/90 (*v/v*), while in PIM MeOH/MeCN 70/30 and 30/70 (*v/v*), all containing 0.1%(*v/v*) TEAA eluents were employed. Data presented in Table S2 reveal, that in all cases retention and selectivity decrease with increasing temperature. Resolution in most cases decreased with increasing temperature, but in a few cases, a maximum curve was registered for R_S with increasing temperature.

When calculating thermodynamic parameters (based on Eq. 2.) except for analyte **6**, all of the plots of ln α *vs. 1/T* could be fitted with straight lines with good correlation coefficients ($R^2 > 0.97$). According to the data in Table 1 the $\Delta(\Delta H^{\circ})$ and $\Delta(\Delta S^{\circ})$ exhibit negative values in all cases. The negative $\Delta(\Delta H^{\circ})$ and $\Delta(\Delta S^{\circ})$ values mean a stronger complex formation between the selector and the second eluted enantiomer, while the negative entropy was less favorable for enantioseparation. At a given mobile phase composition, the non-fluorinated analog (**2**) possesses the most negative $\Delta(\Delta H^{\circ})$ and $\Delta(\Delta S^{\circ})$ values. Analyte **6**, which contains an electron-withdrawing (F-atom) and an electron-donating moiety (methyl group), in most cases, exhibited different behavior. As Fig. 6 illustrates the ln α *vs. 1/T* plots could only be fitted with exponential curves, suggesting different overall binding situations in the limited temperature ranges. Based on the data presented in Table 1, it can be stated that under RP conditions the $\Delta(\Delta H^{\circ})$ and $\Delta(\Delta S^{\circ})$ values are considerably affected by the eluent composition. In both eluent systems markedly more negative $\Delta(\Delta H^{\circ})$ and $\Delta(\Delta S^{\circ})$ values were obtained in eluents with higher H_2O content. Unfortunately, in PIM no enantiorecognition could be achieved for analytes **4** and **5**, while in the case of analyte **6** a distinct behavior was observed, as mentioned above. The rather limited data show more negative $\Delta(\Delta H^{\circ})$ and $\Delta(\Delta S^{\circ})$ values with higher MeCN content, as we described in the case of *Cinchona* alkaloid-based CSPs [12].

On **CF6-P-3.0** CSP the effect of temperature on the enantioseparation was studied with a mobile phase of MeOH/MeCN 10/90 (*v/v*) containing 0.3%(*v/v*) TFA and 0.2%(*v/v*) TEA (Table 2 and Table S3). The analytes behave similarly that in the case of **V-3.0** CSP, *i.e.,* k_1, α, and R_S

Table 1
Effects of eluent composition on the thermodynamic parameters of analytes **2–6** on VancoShell (**V-3.0**) CSP.

Analyte	Temp. range (°C)	-Δ (ΔH^0) (kJ mol^{-1})		-Δ (ΔS^0) (J mol^{-1} K^{-1})		-Δ (ΔG^0)$_{298\ K}$ (kJ mol^{-1})		T_{iso} (°C)		Q	
A, Mobile phase H_2O/MeOH (*v/v*)											
		70/30	10/90	70/30	10/90	70/30	10/90	70/30	10/90	70/30	10/90
2	5–50	5.69	4.26	14.64	10.04	1.33	1.26	115.6	150.8	1.30	1.42
3	5–50	3.23	3.04	8.80	8.28	0.60	0.57	93.4	94.1	1.23	1.23
4	5–40	1.72	–	4.67	–	0.33	–	95.0	–	1.24	–
5	5–30	2.28	–	6.55	–	0.32	–	74.5	–	1.17	–
B, Mobile phase H_2O/MeCN (*v/v*)											
		70/30	10/90	70/30	10/90	70/30	10/90	70/30	10/90	70/30	10/90
2	5–50	7.16	4.62	19.62	13.12	1.31	0.70	91.8	78.7	1.22	1.18
3	5–50	3.79	2.33	10.50	6.58	0.66	0.37	88.3	90.99	1.21	11.19
4	5–50	3.94*	1.19	12.85*	3.28	0.11*	0.21	33.33*	88.28	1.03*	1.21
5	5–50	–	0.80	–	2.27	–	0.12	–	79.56	–	1.18
C, Mobile phase MeOH/MeCN (*v/v*)											
		70/30	30/70	70/30	30/70	70/30	30/70	70/30	30/70	70/30	30/70
2	10–50	2.54	2.56	6.64	6.81	0.61	0.51	117.6	100.6	1.31	1.25
3	5–50	1.39	1.53	3.66	4.02	0.30	0.33	107.5	106.8	1.28	1.28

Chromatographic conditions: column, VancoShell (**V-3.0**); mobile phase, **A**, H_2O/MeOH 70/30 (*v/v*) and H_2O/MeOH 10/90 (*v/v*); **B,** H_2O/MeCN 70/30 (*v/v*) and H_2O/MeCN 10/90 (*v/v*); **C,** MeOH/MeCN 70/30 (*v/v*) and MeOH/MeCN 30/70 (*v/v*) all containing 0.1% TEAA; detection, 215 nm; ln α *vs. 1/T* curves; T_{iso}, temperature where the enantioselectivity cancels; $Q = \Delta(\Delta H^{\circ})/298\ x\ \Delta(\Delta S^{\circ})$

* temperature range: 5–25 °C

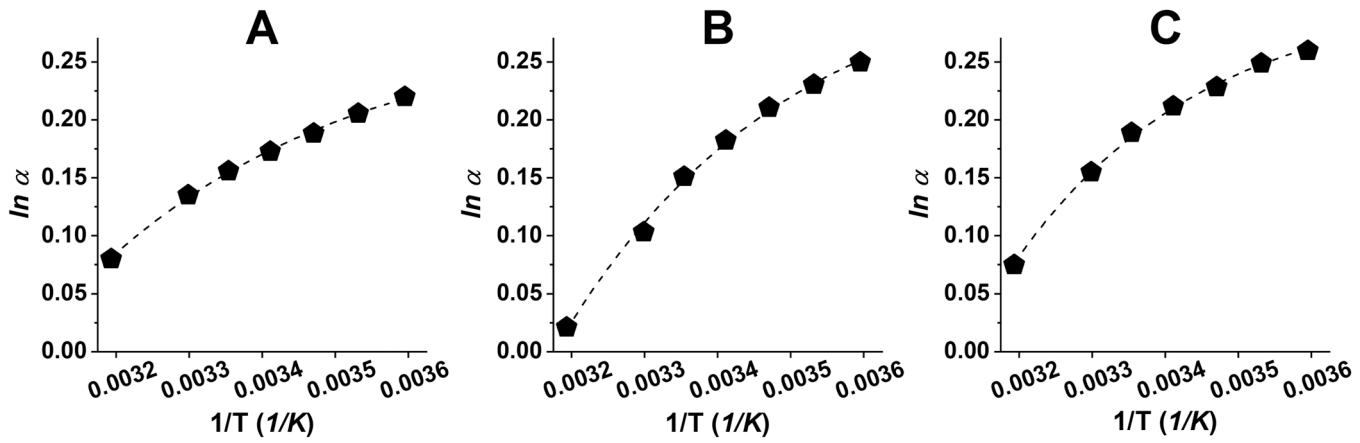

Fig. 6. ln α *vs.* 1/T curves for analyte **6** on VancoShell CSP**,** Chromatographic conditions: column, VancoShell **V-3.0**; mobile phase, **A**, H_2O/MeOH/TEAA, 70/30/0.1 (*v/v/v*), **B**, H_2O/MeCN, 70/30 (*v/v/v*) ***C***, MeOH/MeCN, 30/70/0.1 (*v/v/v*); detection, 215 nm; flow rate, 0.3 ml min^{-1}; temperature, 5–50 °C; symbol analyte **6**, ⬟.

Table 2
Thermodynamic parameters determined on LarichShell-P (**CF6-P-3.0**) CSP.

Compound	$-\Delta$ ($\Delta H°$) (kJ mol^{-1})	$-\Delta$ ($\Delta S°$) (J mol^{-1} K^{-1})	$-\Delta$ $(\Delta G°)_{298\ K}$ (kJ mol^{-1})	T_{iso} (°C)	*Q*
1	2.62	7.51	0.38	75.8	1.17
2	1.60	4.82	0.16	58.6	1.11
3	1.26	3.78	0.13	60.7	1.12
4	1.41	4.34	0.12	51.5	1.04
5	1.49	4.25	0.22	77.5	1.18
6	0.91	2.37	0.20	108.6	1.28
7	0.60	1.25	0.23	207.0	1.61

Chromatographic conditions: column, LarichShell-P (CF6-P-3.0); mobile phase, MeOH/MeCN 10/90 (v/v) containing 0.3%(v/v) FA and 0.2%(v/v) TEA; detection, 215 nm; temperature range, 5–50 °C; ln α *vs.* 1/T curves; Tiso, temperature where the enantioselectivity cancels; Q = Δ(ΔH°)/298 x Δ(ΔS°); temperature range, 5–50 °C

decrease with increasing temperature. Concerning the thermodynamic parameters values were similar in magnitude to those obtained in PIM with **V-3.0** CSP. On **CF6-P-3.0** CSP α- and β-phenylalanine exhibited the most negative $\Delta(\Delta H°)$ and $\Delta(\Delta S°)$ suggesting that the fluoro substitution reduced the differences experienced by the enantiomers in the process of chiral recognition.

To reveal the contribution of the enthalpy and entropy terms to the enantioseparation $Q = \Delta(\Delta H°)/[T \times \Delta(\Delta S°)$; $T = 298$ K] values were also calculated. According to the data in Tables 1 and 2 all the enantiorecognition processes were enthalpically driven, $Q > 1.0$ indicating the relatively higher contribution of enthalpy to the free energy. For the separation of enantiomers.

an interesting consequence is that there is a temperature, the so-called "isoeluotropic" temperature (T_{iso}), where the two enantiomers coelute since entropy and enthalpy changes compensate each other. In this study, in all cases T_{iso} was outside the studied temperature range (Tables 1 and 2).

4. Conclusions

Applying teicoplanin-, teicoplanin aglycone-, vancomycin-, *tert.*-butylcarbamate quinine-, and cyclofructan-6-based CSPs under RP and PI conditions, the vancomycin- and the cyclofructan-6-based CSPs were found to exhibit sufficient effectiveness in the enantiomeric separation of α-phenylalanine, β-phenylalanine and its fluorinated analogs. Baseline separation could be achieved with vancomycin-based CSP for four analytes, with cyclofructan-6-based CSP for two analytes, while with teicoplanin aglycone-based CSP for one analyte. In the case of vancomycin-based CSP, the hydrophobic chromatographic behavior observed with increasing water content is explained by the decreased solvation shell of the ionized analytes and selector. The high increase in retention factors obtained for all analytes with increased MeCN content in PIM was due to the decreased solubility of the polar analytes. Utilizing the stoichiometric displacement model for a description of a possible ion-exchange mechanism, long-range ionic interactions were found to play a negligible role in the chiral recognition process in the case of vancomycin- and teicoplanin aglycone-based selectors. The cyclofructan-6-based CSP offers a markedly different recognition mechanism, which led to baseline separation for the studied analytes in the PIM and a reversal in the enantiomeric elution order. Under PIM conditions, with increasing MeCN content, improved selectivity was observed, suggesting that hydrogen bonding interactions may play a role in the enantiorecognition in the case of cyclofructan-6-based CSP.

The thermodynamic characterization carried out under RP conditions in the case of vancomycin-based CSP revealed that changes in the eluent composition markedly affected the differences in standard enthalpy and standard entropy, without significantly affecting the enthalpy and entropy contributions in the enantioseparation process. Analyses of van Deemter plots in both PIM and RPM confirmed a typical shape with a plate height minima and a flat C-term dependence in most cases. The kinetic characterization provided evidence that the 3.0 i.d. columns outperform the 2.1 mm columns, probably due to wall effects. In this study data were handled without corrections for the extra-column volume of the instrument. The advantageous features of core-shell particles, namely offering the possibility of high-speed enantioseparations and reduced solvent consumption compared to 5-μm particle-based "traditional" columns are worth exploiting.

Declaration of Competing Interest

The authors declare that they have no known competing financial interests or personal relationships that could have appeared to influence the work reported in this paper.

Data availability

Data will be made available on request.

Acknowledgments

This work was supported by National Research, Development and Innovation Office-NKFIA through projects K137607 and K129049. Project no. TKP2021-EGA-32 has been implemented with the support provided by the Ministry of Innovation and Technology of Hungary from the National Research, Development and Innovation Fund, financed

under the TKP2021-EGA funding scheme.

Appendix A. Supporting information

Supplementary data associated with this article can be found in the online version at doi:10.1016/j.jpba.2022.114912.

References

[1] E. Juaristi, V.A. Soloshonok. Enantioselective Synthesis of β-Amino Acids, second ed, Wiley, 2005.

[2] M. Jin, M.A. Fischbach, J. Clardy, A biosynthetic gene cluster for the acetyl-CoA carboxylase inhibitor andrimid, J. Am. Chem. Soc. 128 (2006) 10660–10661, https://doi.org/10.1021/ja063194c.

[3] G. Cardillo, L. Gentilucci, P. Melchiorre, S. Spampinato, Synthesis and binding activity of endomorphin-1 analogues containing β-amino acids, Bioorg. Med. Chem. Lett. 10 (2000) 2755–2758, https://doi.org/10.1016/S0960-894X(00)00562-X.

[4] J. Han, A.M. Remete, L.S. Dobson, L. Kiss, K. Izawa, H. Moriwaki, V.A. Soloshonok, D. O'Hagan, Next generation organofluorine containing blockbuster drugs, J. Fluor. Chem. 239 (2020), 109639, https://doi.org/10.1016/j.jfluchem.2020.109639.

[5] J. Pepin, C. Guern, F. Milord, P.J. Schechter, Difluoromethylornithine for arseno-resistant trypanosoma bruyei gambiense sleeping sickness, Lancet 330 (1987) 1431–1433, https://doi.org/10.1016/S0140-6736(87)91131-7.

[6] J.E. Wolf, D. Shander, F. Huber, J. Jackson, C.-S. Lin, B.M. Mathes, K. Schrode, Randomized, double-blind clinical evaluation of the efficacy and safety of topical eflornithine HCl 13.9% cream in the treatment of women with facial hair, Int. J. Dermatol. 46 (2007) 94–98, https://doi.org/10.1111/j.1365-4632.2006.03079.x.

[7] I. Ilisz, A. Péter, W. Lindner, State-of-the-art enantioseparations of natural and unnatural amino acids by high-performance liquid chromatography, TrAC Trends Anal. Chem. 81 (2016) 11–22, https://doi.org/10.1016/j.trac.2016.01.016.

[8] G.K.E. Scriba, Chiral Separations, Springer New York, New York, NY, 2019, https://doi.org/10.1007/978-1-4939-9438-0.

[9] J.M. Lin, T. Hobo, Inspection of the reversal of enantiomer migration order in ligand exchange micellar electrokinetic capillary chromatography, Biomed. Chromatogr. 15 (2001) 207–211, https://doi.org/10.1002/BMC.63.

[10] T. Tonoi, A. Nishikawa, T. Yajima, H. Nagano, K. Mikami, Fluorous substituent-based enantiomer and diastereomer separation: orthogonal use of HPLC columns for the synthesis of nonproteinogenic polyfluoro amino acids and peptides, Eur. J. Org. Chem. 2008 (2008) 1331–1335, https://doi.org/10.1002/ejoc.200701052.

[11] G. Lajkó, T. Orosz, L. Kiss, E. Forró, F. Fülöp, A. Péter, I. Ilisz, High-performance liquid chromatographic enantioseparation of fluorinated cyclic β3 -amino acid derivatives on polysaccharide-based chiral stationary phases. Comparison with nonfluorinated counterparts, Biomed. Chromatogr. 30 (2016) 1441–1448, https://doi.org/10.1002/bmc.3702.

[12] G. Németi, R. Berkecz, S. Shahmohammadi, E. Forró, W. Lindner, A. Péter, I. Ilisz, Enantioselective high-performance liquid chromatographic separation of fluorinated ß- phenylalanine derivatives utilizing Cinchona alkaloid-based ion-exchanger chiral stationary phases, J. Chromatogr. A (2022), 462974, https://doi.org/10.1016/j.chroma.2022.462974.

[13] C.L. Barhate, L.A. Joyce, A.A. Makarov, K. Zawatzky, F. Bernardoni, W.A. Schafer, D.W. Armstrong, C.J. Welch, E.L. Regalado, Ultrafast chiral separations for high throughput enantiopurity analysis, Chem. Commun. 53 (2017) 509–512, https://doi.org/10.1039/C6CC08512A.

[14] G.L. Losacco, H. Wang, I.A. Haidar Ahmad, J. Dasilva, A.A. Makarov, I. Mangion, F. Gasparrini, M. Lämmerhofer, D.W. Armstrong, E.L. Regalado, Enantioselective UHPLC screening combined with in silico modeling for streamlined development of ultrafast enantiopurity assays, Anal. Chem. 94 (2022) 1804–1812, https://doi.org/10.1021/acs.analchem.1c04585.

[15] C. West, Recent trends in chiral supercritical fluid chromatography, TrAC Trends Anal. Chem. 120 (2019), 115648, https://doi.org/10.1016/j.trac.2019.115648.

[16] D.C. Patel, Z.S. Breitbach, M.F. Wahab, C.L. Barhate, D.W. Armstrong, Gone in seconds: praxis, performance, and peculiarities of ultrafast chiral liquid chromatography with superficially porous particles, Anal. Chem. 87 (2015) 9137–9148, https://doi.org/10.1021/acs.analchem.5b00715.

[17] O.H. Ismail, M. Antonelli, A. Ciogli, M. De Martino, M. Catani, C. Villani, A. Cavazzini, M. Ye, D.S. Bell, F. Gasparrini, Direct analysis of chiral active pharmaceutical ingredients and their counterions by ultra high performance liquid chromatography with macrocyclic glycopeptide-based chiral stationary phases, J. Chromatogr. A 1576 (2018) 42–50, https://doi.org/10.1016/j.chroma.2018.09.029.

[18] J. Yu, M. Wey, S.K. Firooz, D.W. Armstrong, Ionizable cyclofructan 6-based stationary phases for hydrophilic interaction liquid chromatography using superficially porous particles, 2021 849, Chromatographia 84 (2021) 821–832, https://doi.org/10.1007/S10337-021-04063-6.

[19] K. Lomsadze, G. Jibuti, T. Farkas, B. Chankvetadze, Comparative high-performance liquid chromatography enantioseparations on polysaccharide based chiral stationary phases prepared by coating totally porous and core–shell silica particles, J. Chromatogr. A 1234 (2012) 50–55, https://doi.org/10.1016/j.chroma.2012.01.084.

[20] D.C. Patel, Z.S. Breitbach, J.J. Yu, K.A. Nguyen, D.W. Armstrong, Quinine bonded to superficially porous particles for high-efficiency and ultrafast liquid and supercritical fluid chromatography, Anal. Chim. Acta 963 (2017) 164–174, https://doi.org/10.1016/j.aca.2017.02.005.

[21] K. Schmitt, U. Woiwode, M. Kohout, T. Zhang, W. Lindner, M. Lämmerhofer, Comparison of small size fully porous particles and superficially porous particles of chiral anion-exchange type stationary phases in ultra-high performance liquid chromatography: effect of particle and pore size on chromatographic efficiency and kinetic, J. Chromatogr. A 1569 (2018) 149–159, https://doi.org/10.1016/j.chroma.2018.07.056.

[22] R. Berkecz, G. Németi, A. Péter, I. Ilisz, Liquid chromatographic enantioseparations utilizing chiral stationary phases based on crown ethers and cyclofructans, Molecules 26 (2021) 4648, https://doi.org/10.3390/molecules26154648.

[23] R. Berkecz, D. Tanács, A. Péter, I. Ilisz, Enantioselective liquid chromatographic separations using macrocyclic glycopeptide-based chiral selectors, Molecules 26 (2021) 3380, https://doi.org/10.3390/molecules26113380.

[24] A. Cavazzini, G. Nadalini, F. Dondi, F. Gasparrini, A. Ciogli, C. Villani, Study of mechanisms of chiral discrimination of amino acids and their derivatives on a teicoplanin-based chiral stationary phase, J. Chromatogr. A 1031 (2004) 143–158, https://doi.org/10.1016/j.chroma.2003.10.090.

[25] E. Forró, T. Paál, G. Tasnádi, F. Fülöp, A new route to enantiopure β-aryl-substituted β-amino acids and 4-aryl-substituted β-lactams through lipase-catalyzed enantioselective ring cleavage of β-lactams, Adv. Synth. Catal. 348 (2006) 917–923, https://doi.org/10.1002/adsc.200505434.

[26] S. Shahmohammadi, F. Fülöp, E. Forró, Efficient synthesis of new fluorinated β-amino acid enantiomers through lipase-catalyzed hydrolysis, Molecules 25 (2020) 5990, https://doi.org/10.3390/molecules25245990.

[27] W. Kopaciewicz, M.A. Rounds, J. Fausnaugh, F.E. Regnier, Retention model for high-performance ion-exchange chromatography, J. Chromatogr. A 266 (1983) 3–21, https://doi.org/10.1016/S0021-9673(01)90875-1.

[28] P. Sun, C. Wang, Z.S. Breitbach, Y. Zhang, D.W. Armstrong, Development of new HPLC chiral stationary phases based on native and derivatized cyclofructans, Anal. Chem. 81 (2009) 10215–10226, https://doi.org/10.1021/AC902257A/SUPPL_FILE/AC902257A_SI_001.PDF.

[29] D. Roy, D.W. Armstrong, Fast super/subcritical fluid chromatographic enantioseparations on superficially porous particles bonded with broad selectivity chiral selectors relative to fully porous particles, J. Chromatogr. A 1605 (2019), 360339, https://doi.org/10.1016/j.chroma.2019.06.060.

[30] T. Orosz, E. Forró, F. Fülöp, W. Lindner, I. Ilisz, A. Péter, Effects of N-methylation and amidination of cyclic β-amino acids on enantioselectivity and retention characteristics using Cinchona alkaloid- and sulfonic acid-based chiral zwitterionic stationary phases, J. Chromatogr. A 1535 (2018) 72–79, https://doi.org/10.1016/j.chroma.2017.12.070.

[31] N. Grecsó, E. Forró, F. Fülöp, A. Péter, I. Ilisz, W. Lindner, Combinatorial effects of the configuration of the cationic and the anionic chiral subunits of four zwitterionic chiral stationary phases leading to reversal of elution order of cyclic β3-amino acid enantiomers as ampholytic model compounds, J. Chromatogr. A 1467 (2016) 178–187, https://doi.org/10.1016/j.chroma.2016.05.041.

[32] I. Ilisz, A. Bajtai, W. Lindner, A. Péter, Liquid chromatographic enantiomer separations applying chiral ion-exchangers based on Cinchona alkaloids, J. Pharm. Biomed. Anal. 159 (2018) 127–152, https://doi.org/10.1016/j.jpba.2018.06.045.

[33] D. Tanács, R. Berkecz, A. Misicka, D. Tymecka, F. Fülöp, D.W. Armstrong, I. Ilisz, A. Péter, Enantioseparation of ß-amino acids by liquid chromatography using core-shell chiral stationary phases based on teicoplanin and teicoplanin aglycone, J. Chromatogr. A 1653 (2021), 462383, https://doi.org/10.1016/j.chroma.2021.462383.

[34] D. Folprechtová, K. Kalíková, K. Kadkhodaei, C. Reiterer, D.W. Armstrong, E. Tesařová, M.G. Schmid, Enantioseparation performance of superficially porous particle vancomycin-based chiral stationary phases in supercritical fluid chromatography and high performance liquid chromatography; applicability for psychoactive substances, J. Chromatogr. A 1637 (2021), https://doi.org/10.1016/j.chroma.2020.461846.

[35] L.D. Asnin, M.V. Stepanova, Van't Hoff analysis in chiral chromatography, J. Sep. Sci. 41 (2018) 1319–1337, https://doi.org/10.1002/jssc.201701264.